

# Evolutionary Retrosynthetic Route Planning

Yan Zhang<sup>1,2</sup>, Hao Hao<sup>3</sup>, Xiao He<sup>1,4</sup>, Shuanhu Gao<sup>1,4</sup> and Aimin Zhou<sup>1,2,\*</sup>

<sup>1</sup>Shanghai Frontiers Science Center of Molecule Intelligent Syntheses, Shanghai, 200062, China

<sup>2</sup>School of Computer Science and Technology, East China Normal University, Shanghai, 200062, China

<sup>3</sup>Institute of Natural Sciences, Shanghai Jiao Tong University, Shanghai, 200240, China

<sup>4</sup>School of Chemistry and Molecular Engineering, East China Normal University, Shanghai, 200240, China

arXiv:2310.05186v1 [cs.AI] 8 Oct 2023

**Abstract**—Molecular retrosynthesis is a significant and complex problem in the field of chemistry, however, traditional manual synthesis methods not only need well-trained experts but also are time-consuming. With the development of big data and machine learning, artificial intelligence (AI) based retrosynthesis is attracting more attention and is becoming a valuable tool for molecular retrosynthesis. At present, Monte Carlo tree search is a mainstream search framework employed to address this problem. Nevertheless, its search efficiency is compromised by its large search space. Therefore, we propose a novel approach for retrosynthetic route planning based on evolutionary optimization, marking the first use of Evolutionary Algorithm (EA) in the field of multi-step retrosynthesis. The proposed method involves modeling the retrosynthetic problem into an optimization problem, defining the search space and operators. Additionally, to improve the search efficiency, a parallel strategy is implemented. The new approach is applied to four case products, and is compared with Monte Carlo tree search. The experimental results show that, in comparison to the Monte Carlo tree search algorithm, EA significantly reduces the number of calling single-step model by an average of 53.9%. The time required to search three solutions decreased by an average of 83.9%, and the number of feasible search routes increases by 5 times. The source code is available at <https://github.com/ilog-ecnu/EvoRRP>.

**Index Terms**—Retrosynthesis, Evolutionary optimization, Parallel computation.

## I. INTRODUCTION

Molecular retrosynthesis is of great importance in various fields [1], [2], including drug synthesis and catalyst design. It enables rapid determination of potential pathways and starting materials for the synthesis of target compounds, while also providing essential guidance for synthesis routes. Retrosynthetic process is divided into two processes: single-step retrosynthesis and multi-step search process. The single-step retrosynthesis process involves breaking down an organic molecule into its original reactants. As illustrated in Fig. 1, the retrosynthetic route for target product is generated using this method. The intermediate molecules,  $R^1$  and  $W^1$ , are obtained through the single-step model with the input target product  $P$ .  $W^1$  belongs to the set  $\Psi$ , which represents the building block dataset containing commercially available molecules, serving as the terminal reactant database. The process continues by selecting  $R^1$  as input for the single-step model, and this cycle repeats until all products belong to  $\Psi$ , forming a multi-step retrosynthetic reactions.

In recent years, neural network (NN), particularly architectures like transformers, has played a crucial role in advancing

this field. A transformer architecture [3] has become a common choice for single-step retrosynthesis tasks. It has achieved significant advancements and greatly improved search effectiveness, leading to remarkable progress in the field of retrosynthesis. Currently, researchers are focusing on multi-step retrosynthetic route planning [4]. This involves a combination of single-step retrosynthetic models based on transformer or convolutional neural network, along with a multi-step Monte Carlo tree search framework. This approach has emerged as a valuable asset in the field of chemistry. It empowers chemists to expedite the synthesis of novel compounds with enhanced efficiency and precision, opening new vistas of exploration and discovery in the vast realm of chemical synthesis.

Monte Carlo Tree Search (MCTS) is a decision-making algorithm initially applied to multi-step retrosynthesis by Marvin et al. [1]. They used a neural network for single-step retrosynthesis, which is an end-to-end sequence generation effort, and MCTS for route search effort. The neural network was trained on a large dataset of known organic reactions to predict the outcome of a given chemical reaction. MCTS was used to search for the optimal synthetic route by exploring the possible chemical transformations that could be applied to the target molecule, evaluating the likelihood of each transformation using the neural network, and selecting the best one to apply. The advantage of this approach is that it can efficiently explore a large search space and find a good solution, while the neural network can provide accurate predictions of chemical reactions. Lin et al. [3] also applied MCTS with a heuristic scoring function for multi-step retrosynthetic route planning. MCTS is a powerful algorithm for decision making in complex problems, however, its effectiveness and efficiency depend on several factors such as the complexity of the problem, the branching factor of the tree, the number of simulations required, and the computational resources available. Therefore, researchers must carefully design the algorithm and its parameters to achieve the desired results. While MCTS has many advantages in decision-making problems with a large number of possible actions and states, there are also a few drawbacks to consider. Firstly, it may not work well for games or problems that have specific structures or constraints. Secondly, the search efficiency of MCTS is not very high due to its requirement of a large search space during the exploration process. Lastly, MCTS can be computationally expensive, particularly when the branching factor of the tree is high or when a large number of simulations are needed. While MCTS can be parallelized [5], it is not commonly used

Corresponding author: Aimin Zhou (amzhou@cs.ecnu.edu.cn).

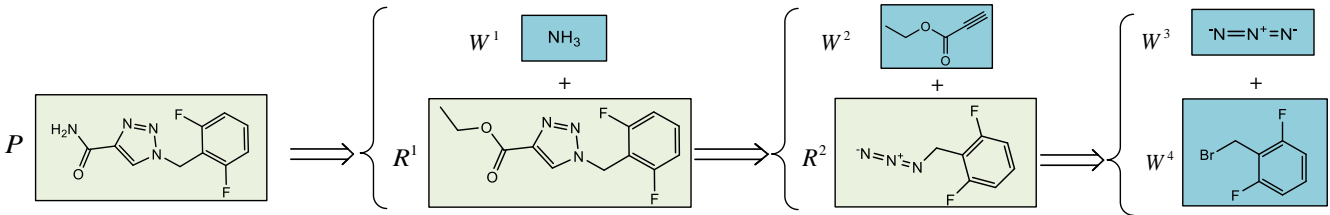


Fig. 1. Multi-step retrosynthetic route from target product  $P$  to ingredients  $W$ . The single-step retrosynthetic process is iteratively employed until all  $W$  belong to the building block dataset.

in the context of retrosynthetic route planning.

In summary, we propose a method for retrosynthetic route planning using evolutionary optimization, which can purposefully find the optimal solution while adhering to the constraints of the objective function. The method defines the search space and limits the search scope, thereby reducing the generation of infeasible solutions. Moreover, the proposed method employs parallel computation to reduce the search time and improve search efficiency and the number of search routes. The contributions of this paper can be summarized as follows:

- We introduce a novel method for retrosynthetic problem, which can be solved by Evolutionary Algorithm (EA), marking the first use of EA in the field of multi-step retrosynthesis.
- The proposed method greatly reduces the single-step model calls, decreasing the frequency of generating invalid solutions, and improving search efficiency.
- Additionally, a parallel strategy is implemented to improve the search efficiency during the searching process.
- Our proposed method is executed on four case products, and performs better than Monte Carlo tree search method.

The structure of the subsequent chapters is as follows. Section 2 provides an overview of single-step retrosynthesis, multi-step retrosynthesis, and evolutionary algorithms. In Section 3, the proposed method is presented in detail, followed by a series of comparative experiments in Section 4. The final Section concludes the paper by summarizing its key findings and contributions.

## II. RELATED WORK

### A. Single-step retrosynthesis

Single-step retrosynthesis can be categorized into template-based [6]–[8], template-free [3], [9]–[11], and semi-template [12]–[14] methods. Template-based retrosynthesis [15] employs a pre-defined set of reaction templates to guide retrosynthetic analysis. These templates are based on frequently used organic synthesis reactions and can suggest possible starting materials for a desired target molecule. For instance, if the target molecule has a carbonyl group, the template-based approach may recommend using a nucleophilic addition reaction to introduce the carbonyl group and then working backwards to identify the precursor molecules for the reaction. Though this approach yields high accuracy, it requires a considerable amount of computation. Furthermore, the rule cannot cover the response range completely, and its scalability is limited. Template-based retrosynthetic reactions utilize reaction rules

that may lead to reactivity conflicts. To deal with this, deep neural networks [16] have been used to resolve this problem. Computer-assisted synthesis planning (CASP) [17] was also gaining attention and molecular similarity has been found to be an effective metric for proposing and ranking single-step retrosynthetic disconnections. Deep learning-based method [18], which combine local reactivity and global attention mechanisms, was commonly used for retrosynthetic reaction prediction.

Template-free retrosynthesis [19] is a more flexible approach that does not rely on pre-defined reaction templates. Instead, it involves breaking down the target molecule into smaller fragments based on the functional groups present and then considering possible ways to connect these fragments. This open-ended approach can be useful for exploring a wider range of possible synthetic pathways. However, the accuracy of this approach is not high, especially when the reaction type is unknown, although its scalability is good. Template-free methods, on the other hand, have high scalability but lower accuracy compared to template-based methods. Retroformer [20] used a novel differentiable MCTS method to directly predict products from reactants, achieving end-to-end retrosynthesis. RetroPrime [21] combined global and local contextual information, employed a multi-layer transformer architecture, and used a multi-task learning strategy to improve the accuracy and robustness of retrosynthesis prediction. Besides transformer, graph-based truncated attention (GTA) model [22] employed a truncated attention mechanism to handle interactions between different nodes and combined a reaction library with graph neural networks for retrosynthetic prediction.

Several semi-template-based approaches [23], [24] also exist, such as a molecular graph-enhanced transformer model [25] that represented molecular structures in graph form and used graph-based self-attention mechanisms to handle interactions between different atoms in the molecule. Additionally, the model used an adaptive structural embedding method to enhance its ability to model molecular structures.

### B. Multi-step search process

Multi-step retrosynthetic reaction involves a series of consecutive single-step retrosynthesis to gradually break down the target molecule, starting from the target molecule and undergoing transformations of multiple intermediate compounds, ultimately yielding simpler starting materials. It emphasizes the requirement for multiple reaction steps to accomplish the decomposition of the target molecule, with each step

serving as a crucial component of the retrosynthesis. One such approach is the game tree search [26], which generated new drug molecules by searching for potential reaction paths. This method combined traditional rule-based and deep learning methods and used a reinforcement learning algorithm, called game tree search, to guide the drug molecule construction process. Another method is the one proposed by Klucznik et al. [27], which planned the synthesis path and predicted possible side reactions based on the structural characteristics and synthetic difficulty of the target compounds. However, this approach had poor performance in terms of speed of synthesis. To solve this issue, a computer program [2] was developed to predict the optimal reaction conditions for target compounds, which was then used to control the robotic platform to perform multiple reactions simultaneously in flow reactors. Retro\* [28] combined neural networks with MCTS to generate synthetic pathways. Additionally, a computational framework [29], integrating a reaction database, a generative model, and an evaluation function, was developed to guide the MCTS-based search for green synthetic pathways. The Reinforcement Learning (RL) algorithm was employed to learn from previous MCTS searches and update the evaluation function to improve search efficiency. These methods demonstrate the potential of computer-assisted synthesis planning in improving the efficiency and accuracy of chemical reactions.

### C. Evolutionary optimization

Evolutionary algorithm (EA) is a kind of population-based optimization algorithm, through the selection of the fittest among individuals to select offspring, so as to solve some complex optimization problems. There are several operators that can be used to generate new solutions, such as genetic algorithm (GA) [30], the differential evolution (DE) [31], the particle swarm optimization (PSO) [32]. Other approaches include evolution strategies (ES) [33], evolutionary programming (EP) [34], [35] and genetic programming (GP) [36], and estimation of distribution algorithms (EDA) [37]. EDA used machine learning methods to generate new solutions and can converge to the global optimum faster than traditional EA frameworks. EDA can be classified into three types: univariate EDA [38], multivariate EDA [39]–[44] and multi-objective EDA [45]–[48]. Population-Based Incremental Learning (PBIL) [49] was a representative univariate EDA that combined genetic search-based function optimization and competitive learning. It used a probabilistic model to generate candidate solutions and encouraged diversity by introducing random perturbations. Pelikan et al. [50] proposed a probabilistic modeling approach, a kind of multivariate EDA method, based on Bayesian networks to solve the linkage problem and estimate the joint probability distribution of variables in a high-dimensional search space. BMDA [51] was another well-known multivariate EDA method that estimates the joint probability distribution of decision variables and used this information to guide the search for the global optimum. Naive MIDEA [52] was a multi-objective optimization algorithm that balanced convergence and diversity by using a fitness assignment scheme based on the distance between solutions. It also incorporated a crowding

distance measure to promote diversity in the population. A hybrid Bayesian optimization algorithm [53] was proposed to combine Gaussian process with tree-structure Bayesian optimization and introduce the variance adaptive mechanism, which can solve high-dimensional complex function optimization problems. In summary, EDA has the ability to learn the problem structure and is suitable for solving real optimization problems with special situations. There are also some typical application cases [54]–[56] of evolutionary optimization. For instance, In the study by Weber et al. [56], they proposed a method to process multi-component reactions using evolutionary search methods for drug discovery. Multi-component reactions (MCRs) offer a novel method for synthesizing a wide range of compounds and compound libraries efficiently. Once considered merely a chemistry curiosity, MCRs are now acknowledged for their growing significance in drug discovery, particularly in lead discovery and optimization. This evolutionary search method primarily emphasizes in silico filtering, but one of its limitations is the lack of integration with deep learning techniques.

## III. PROPOSED METHOD

This section initiates by framing the retrosynthetic problem as a tree search problem, where the objective is to find a sequence of routes leading from the root node to leaf nodes. Then the evolutionary algorithm efficiently solves the tree search problem.

### A. Retrosynthetic problem

In retrosynthetic analysis, reactions similar to Eq. 1a are known as forward synthesis reactions. In this equation, a complex molecule  $R$  and a simple molecule  $W$  act as reactants, resulting in the formation of molecule  $P$ . On the other hand, Eq. 1b is termed as single-step retrosynthetic reactions, representing the reverse of the forward synthesis reaction and forming the basis of retrosynthetic analysis. The objective of retrosynthetic analysis is to identify potential precursors or starting materials for synthesizing the target molecule  $P$  using these simpler molecules  $W$ , which are often found in nature or obtained through standard reactions. As a result, the primary focus in single-step retrosynthetic analysis is on selecting a structurally more complex molecule  $R$  for further retrosynthetic analysis. The single-step retrosynthesis process can be represented as Eq. 1c,



where  $R$  and  $W$  represent reactants,  $P$  represents product in Eq 1a.

For single-step retrosynthesis, the dataset is structurally expressed as  $\{< P, R >\}$ , where each pair contains the target product  $P$  and the corresponding target reactant  $R$ , represented using SMILES expressions. In this problem, both the input and output are strings (SMILES expressions) [57],

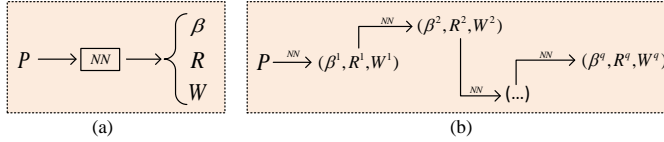


Fig. 2. (a) represents a single-step retrosynthetic process. In this context,  $P$  denotes the target product,  $NN$  expresses single-step model,  $R$  and  $W$  represent the reactants, where  $W \in \Psi$ ,  $\Psi$  represents building block dataset.  $\beta$  signifies the probability of the reactant being involved in the process. (b) represents a multi-step retrosynthetic process, which repeats the single-step retrosynthetic process  $q$  times.

which can be treated as sentences. Therefore, it can be transformed into a sentence-to-sentence translation task falling under the field of Natural Language Processing (NLP). The  $NN$  structural model [3] is commonly employed to address NLP challenges, with the implementation of a transformer structure in this approach. Simultaneously, Fig. 2(a) shows that schematic mathematical formula is employed to describe the graph presented in Fig. 1. This model takes the target product  $P$  as input and generates the corresponding complex molecule  $R$  and simpler molecule  $W$  as output.  $\beta$  signifies the probability of the reactant being involved in the process. The process is simplified in this representation, depicting a single-step retrosynthetic prediction. However, in practice, the execution of the single-step retrosynthetic model can be visualized as shown in Fig. 3. In this structure, the molecule Rufinamide represents the target product  $P$ . The nodes top-1 to top- $k$  represent the  $k$  most probable cases of the target product  $R$  inferred by  $NN$ .  $\beta^i$  indicates the corresponding probability of  $i$ -th possible case.

In multi-step retrosynthesis, the process involves a series of multiple single-step reactions, as illustrated in the simplified diagram shown in Fig. 2(b). The objective of multi-step retrosynthesis is to identify one or more feasible routes from the root node to the leaf nodes. The single-step retrosynthetic model is utilized during the expansion of the tree to explore potential reactions and pathways. For example, in the context of Fig. 4, the path from the root node to the leaf node, connected by the blue lines in the figure, represents a feasible route. The  $k$ -cross tree search facilitates the exploration of potential reaction pathways.

### B. Retrosynthetic optimization model

The number of potential chemical structures for organic molecules can reach an enormous scale, up to about  $10^{60}$  compounds [58]. However, only a much smaller subset of compounds exhibits reasonable structural characteristics. Therefore, constructing a search space that explores the natural distribution of organic structures with structural rationality is a crucial challenge. The search space is defined as the top- $k$  reactants with the highest inferred confidence in the single-step retrosynthetic reaction. The choice of the value  $k$  is crucial as it impacts the search efficiency and the quality of the solutions. If the search space is too small, there is a risk of missing the global optimal solution. Conversely, if the search space is too large, the algorithm will consume more GPU memory and time, potentially leading to local optimality and reduced

efficiency. Due to the vast search space, tree search alone may not be sufficient to effectively solve the problem. Therefore, heuristic algorithms are employed to address this limitation and provide better solutions.

To tackle the retrosynthetic problem, it is converted into an optimization problem resembling tree search. Suppose that a multi-step retrosynthesis involves  $q$  single-step retrosynthesis processes. We use  $(x, r, \beta)$  to represent a multi-step retrosynthesis, where  $x = (x^1, x^2, \dots, x^q)$ , and  $x^i \in \{1, 2, \dots, k\}$  represents the  $x^i$ -th possible output of the  $i$ -th single-step retrosynthesis. Let  $r = (r^1, r^2, \dots, r^q)$  denotes decoding results from  $x$  using single-step retrosynthesis, as shown in Fig. 3, and  $r^i$  represents SMILES expression (eg.,Fc1cccc(F)c1CBr.[N-]=[N+]=[N-]) of the  $i$ -th single-step retrosynthesis.  $\beta = (\beta^1, \beta^2, \dots, \beta^q)$  denotes the corresponding probability of  $r$ . Take  $(< 2, 2, 1 >, < r^1, r^2, r^3 >, < 0.8, 0.9, 0.7 >)$  as an example, there are 3 steps: in the 1st step,  $r^1$  is chosen as the second reactant of  $NN$  with a probability of  $\beta^1=0.8$ ; in the 2nd step,  $r^2$  is chosen as the second reactant of  $NN$  with a probability of  $\beta^2=0.9$ ; in the 3rd step,  $r^3$  is chosen as the first reactant of  $NN$  with a probability of  $\beta^3=0.7$  and it is a known molecule in  $\Psi$ .

To assess the validity of each route within the tree search problem, it is also essential to compare the molecular structure of  $r^q$  with that in  $\Psi$ . The Morgan fingerprint [59], a widely used molecular representation, is utilized to encode the molecular structure. The Morgan fingerprint for  $r^q$  and each molecule in  $\Psi$  can be derived, and their molecular similarity can be calculated using RDKit [60], a popular cheminformatics library. The similarity score is defined as follows:

$$g(x) = \max_{z \in \Psi} \{ \text{RDKit}(x, z) \} \quad (2)$$

The value of  $g(x)$  typically ranges between 0 and 1. In this scenario, the optimization objective shifts towards discovering the maximum value of the objective function. The mathematical expression for objective function is as follows:

$$f(x) = g(x) \times \prod_{i=1}^q \beta^i \quad (3)$$

The process of obtaining the objective function is depicted in Fig. 5.

### C. Evolutionary optimization

In this paper, the proposed method adopts EA as the approach for algorithmic optimization. Prior to utilizing this algorithm, a search space transformation is required, wherein the problem search space is mapped to the variation space. Subsequently, variation, sampling and selection are performed.

1) *Search space transformation*: The EA algorithm employs continuous real numbers for its coding, which necessitates mapping the continuous variation space, denoted as  $y$ , to the discrete search space, denoted as  $x$ . Then, Eq. 3 is used to compute  $f(x)$  for evaluating solutions. The variation space of EA is defined as  $y = (y^1, y^2, \dots, y^q)$ , where  $y^i \in [0, 1)$ . When the variation space is equally divided into  $k$  segments

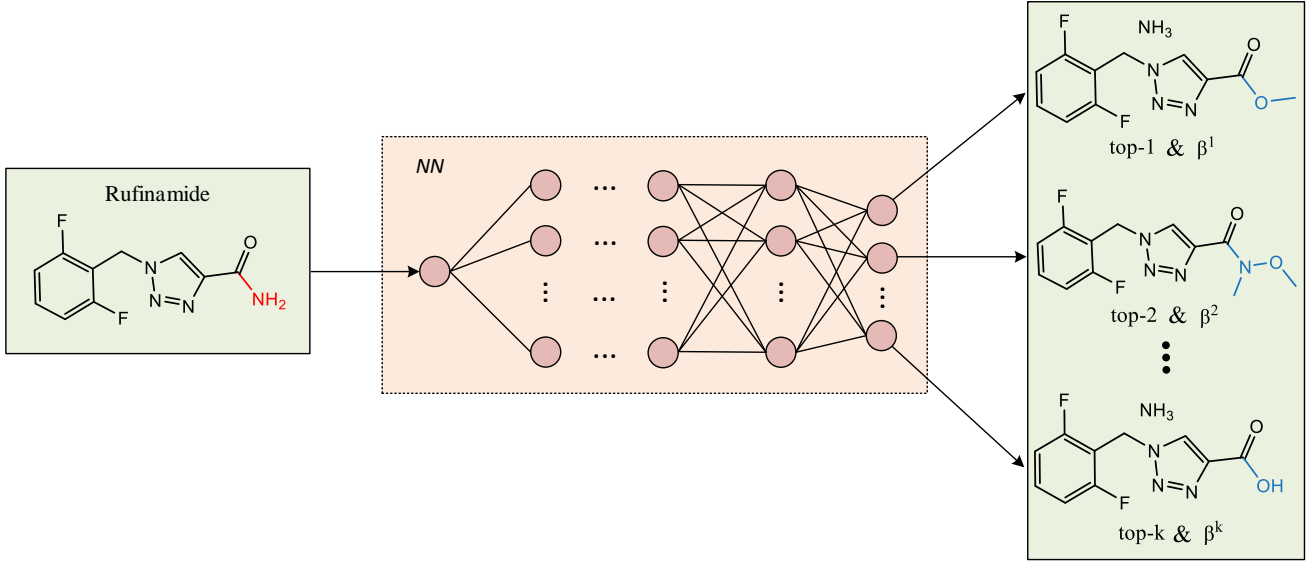


Fig. 3. In the framework of single-step retrosynthetic model, the top- $k$  predicted reactants with the highest confidence, inferred by a neural network ( $NN$ ), are utilized. The  $\beta^i$  represents the probability of generating the corresponding product.

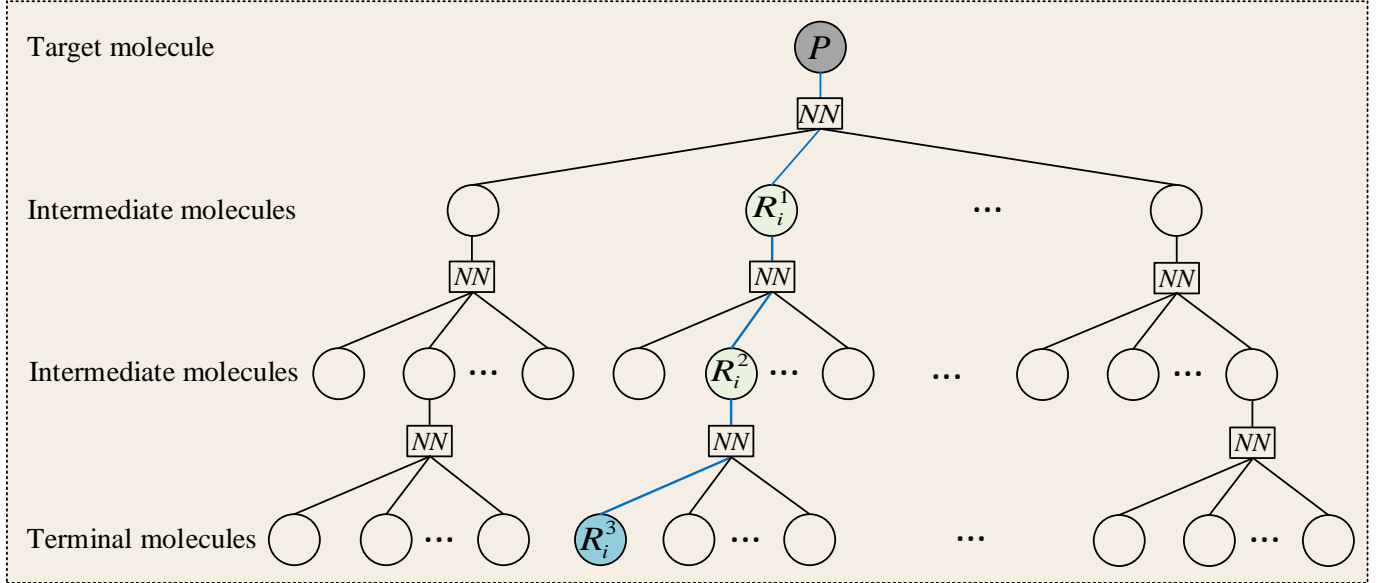


Fig. 4. K-cross search tree structure transformed by multi-step retrosynthesis process. Gray root node represents target product,  $NN$  represents transformer model, blue leaf node stands for raw material in the building block dataset.

ranging from 0 to 1,  $x^i$  can be derived from  $y^i$  using the following mapping:

$$x^i = \lambda \quad \text{if } \frac{\lambda-1}{k} \leq y^i < \frac{\lambda}{k} \quad \lambda \in \{1, 2, \dots, k\} \quad (4)$$

2) *Variation*: The retrosynthetic problem is tackled using the Estimation of Distribution Algorithm (EDA) [61] during the execution of the EA process. EDA operator stands out among other operators as it generates new solutions by sampling from a histogram probabilistic model. This characteristic enables EDA to produce better or more similar solutions and converge faster. The basic framework of the proposed method is depicted in Fig. 6. The process of variation consists

the establishment of the probability model and sample. To construct the probability model, the variation space  $[a^{i,0}, a^{i,M}]$  for the  $i$ -th variable is divided into  $M$  bins, where  $a^{i,0} = 0$  and  $a^{i,M} = 1$  are the boundaries of the bins. Subsequently,  $a^{i,1}$  and  $a^{i,M-1}$  can be set as follows:

$$\begin{aligned} a^{i,1} &= \max \left\{ y_1^{i,\min} - 0.5 \left( y_2^{i,\min} - y_1^{i,\min} \right), a^{i,0} \right\} \\ a^{i,M-1} &= \min \left\{ y_1^{i,\max} + 0.5 \left( y_2^{i,\max} - y_1^{i,\max} \right), a^{i,M} \right\} \end{aligned} \quad (5)$$

where  $y_1^{i,\min}$  and  $y_2^{i,\min}$  are the first and second minimum values, respectively, of the  $i$ -th element among the individuals in the population. Similarly,  $y_1^{i,\max}$  and  $y_2^{i,\max}$  represent the first and second maximum values, respectively, of the  $i$ -th

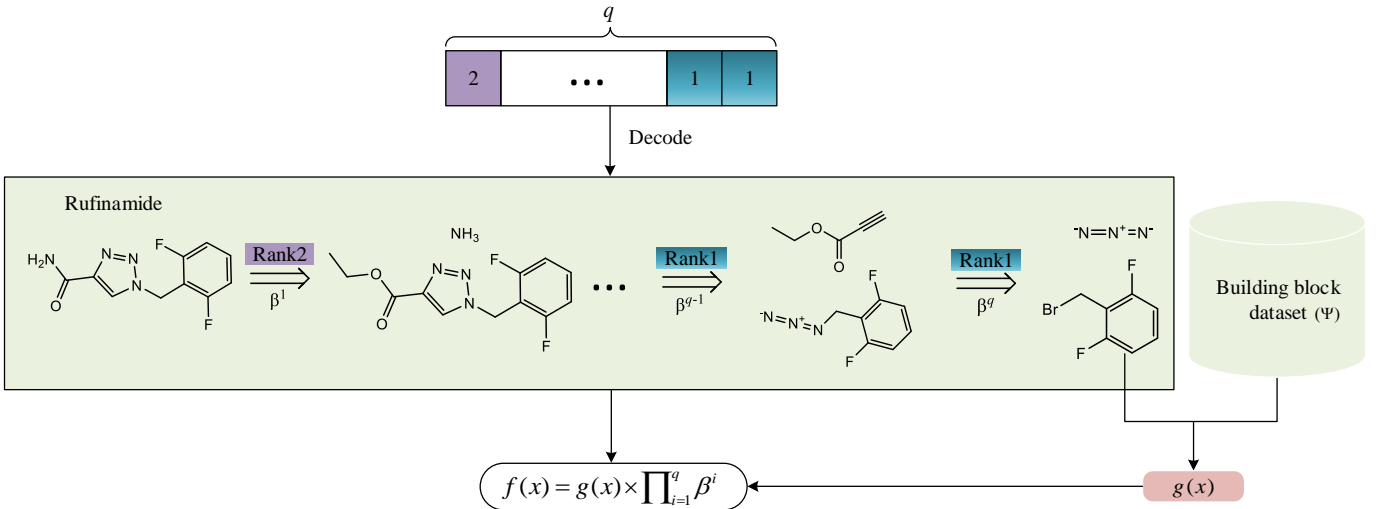


Fig. 5. The basic framework of objective function  $f(x)$ . The value of  $q$  denotes the number of layers from the root node  $P$  to a leaf node, as shown in Fig. 4. The single-step retrosynthesis process can be interpreted as the decoding process.

element among the individuals in the population. The  $M-2$  middle bins are of equal width, with the same size:

$$a^{i,m} - a^{i,m-1} = \frac{1}{M-2} (a^{i,M-1} - a^{i,1}) \quad (6)$$

The values assigned to each bin depend on the number of solutions found within their respective intervals, with lower values assigned to the first and last bins. To ensure that each bin has a chance of being searched,  $C^{i,m}$  is used to represent the number of individuals in the  $m$ -th bin for variable  $y^i$ .

$$C^{i,m} = \begin{cases} C^{i,m} + 1 & \text{if } 1 < m < M \\ 0.1 & \text{if } m = 1, M, \text{ and } a^{i,m} > a^{i,m-1} \\ 0 & \text{if } m = 1, M, \text{ and } a^{i,m} = a^{i,m-1} \end{cases} \quad (7)$$

Then the probability model can be constructed as follows:

$$P^{i,m} = \frac{C^{i,m}}{\sum_{j=1}^M C^{i,j}}. \quad (8)$$

The process of sample is presented in Algorithm 1.

---

**Algorithm 1:** Sample from probability model

---

1 **Input:** probability model  $P(y)$ .  
 2 **Output:** new candidate solution  $y$ .  
 3 **for**  $i = 1, \dots, n$  **do**  
 4     Select a bin  $m$  according to probability model  $P^{i,j}, j = 1, \dots, M$ .  
 5     Randomly select a value  $y^i$  from  $[a^{i,M-1}, a^{i,M}]$  if  $m = M$  or  $[a^{i,m-1}, a^{i,m}]$  if  $m < M$ .  
 6 **end**  
 7 **Return**  $y = (y^1, y^2, \dots, y^q)$ .

---

3) *Decoding and evaluate:* Once new solutions are generated, they are combined with the current solutions. The  $y$ -space is transformed into the  $x$ -space through search space transformation, followed by decoding to obtain  $r$ , which allows for the calculation of  $f(x)$ . The top- $n$  individuals are

then chosen based on  $f(x)$  as the solutions for the subsequent iteration. These steps are repeated until the predetermined stopping criteria are met, such as reaching the maximum number of iterations or fulfilling the convergence condition.

4) *Parallel implementation:* EA is a population-based search method, where each individual in the population is independent and represents a complete retrosynthetic route, making it natural for parallel computation. Leveraging this advantage, parallel EA distributes  $n$  individuals across different GPUs for simultaneous computation, following a specific order:

$$s = j \% m \quad (9)$$

where  $j$  represents the  $j$ -th individual in the population,  $m$  is the number of GPU, then  $s$  represents the remainder of dividing  $j$  by  $m$ . In this case, the  $j$ -th individual is assigned to the  $s$ -th GPU for computation, as shown in Fig. 7.

## IV. EXPERIMENT

In this section, we will begin by introducing the datasets and parameter settings. Next, we will conduct a comparative study using various methods and perform extensive experiments on four case products. Finally, we have provided several charts and conducted corresponding analysis.

### A. Datasets

In this experiment, we performed retrosynthetic route planning for four case products. Two commonly used benchmark datasets, namely USPTO\_50K [62], [63] and USPTO/MIT, were utilized to train single-step retrosynthetic model. The USPTO\_50K dataset was extracted from the patent literature of the United States, while USPTO/MIT was previously employed by Lin et al. [3]. The distribution of reaction classes in the two datasets is presented in Table I. To define the terminal nodes or reactants, the building block dataset [3] is built, which contains 93563 commercially available molecules.

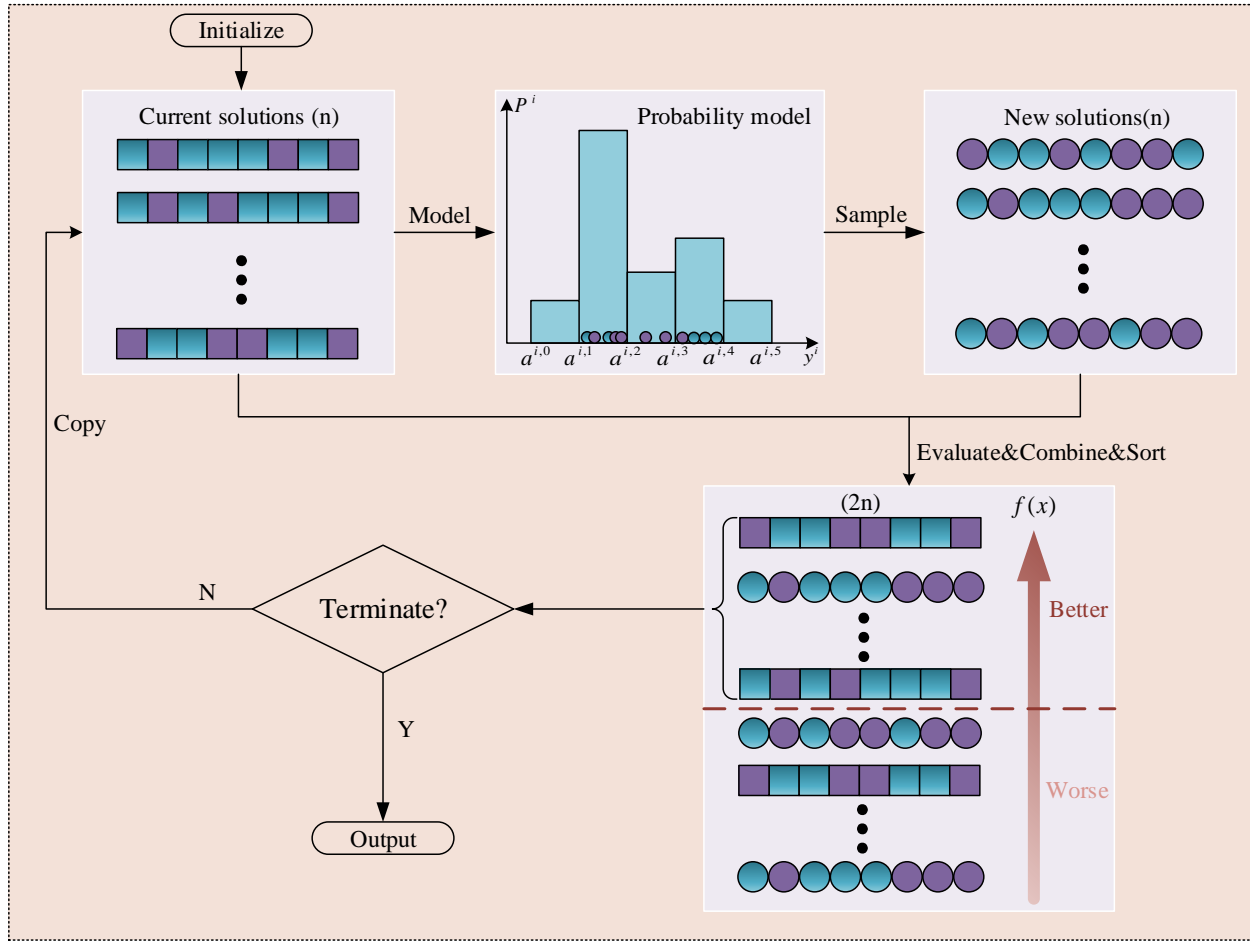


Fig. 6. The framework of the retrosynthetic problem utilizes Evolutionary Algorithm (EA). Within this framework, EDA operator consists of two processes: the establishment of probability model and the sampling, and it is used to generate the new solutions through sampling. The sampled results are then combined with current solutions, sorted by  $f(x)$ , and the first  $n$  individuals are selected as the new solutions for the next iteration.

TABLE I  
DESCRIPTIONS OF TEN REACTION CLASSES AND THE RATIO OF USPTO\_50K AND USPTO\_MIT

Reaction class	Reaction name	USPTO_50k(%)	USPTO_MIT(%)
1	Heteroatom alkylation and arylation	30.3	29.9
2	Acylation and related processes	23.8	24.9
3	C-C bond formation	11.3	13.4
4	Heterocycle formation	1.8	0.7
5	Protections	1.3	0.3
6	Deprotections	16.5	14.1
7	Reductions	9.2	9.4
8	Oxidations	1.6	2.0
9	Functional group interconversion (FGI)	3.7	5.0
10	Functional group addition (FGA)	0.5	0.2

TABLE II

ANALYSIS ON THE NUMBER (MEAN(STD.DEV.))[PERCENTAGE] OF CALLING SINGLE-STEP MODEL FOR MCTS AND EA. PERCENTAGE IN “[·]” EXPRESSES INCREASE OR DECREASE OF EA COMPARED WITH MCTS IN THE SAME COLUMN AND UNDER THE SAME PRODUCT. OVER 30 INDEPENDENT RUNS.

Products	Method	One solution	Two solutions	Three solutions
DemoA	MCTS	1.20e+2(8.34e+1)	1.95e+2(8.34e+1)	2.74e+2(1.12e+2)
DemoB	MCTS	3.81e+2(3.13e+2)	4.56e+2(3.13e+2)	4.89e+2(3.39e+2)
DemoC	MCTS	2.13e+3(1.70e+3)	3.38e+3(2.19e+3)	3.65e+3(2.35e+3)
DemoD	MCTS	4.58e+3(2.77e+3)	4.87e+3(2.07e+3)	4.82e+3(2.00e+3)
DemoA	EA	2.30e+1(1.89e+1)[80.8%↓]	5.85e+1(4.19e+1)[70.0%↓]	8.23e+1(4.45e+1)[70.0%↓]
DemoB	EA	2.48e+1(2.33e+1)[93.5%↓]	6.64e+1(3.87e+1)[85.4%↓]	1.11e+2(5.48e+1)[77.3%↓]
DemoC	EA	2.60e+1(1.45e+1)[98.8%↓]	2.11e+3(1.28e+3)[35.8%↓]	2.41e+3(3.28e+2)[34.0%↓]
DemoD	EA	2.69e+3(1.11e+3)[41.3%↓]	2.69e+3(1.01e+3)[44.8%↓]	3.16e+3(3.45e+2)[34.4%↓]

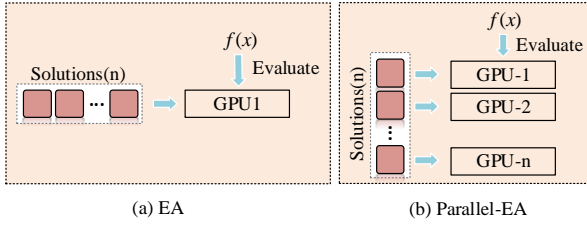


Fig. 7. Parallel computing of EA. The population consists of  $n$  individuals, represented by red squares. In the standard EA, each individual is evaluated sequentially. However, in parallel EA, different individuals can be assigned to separate GPUs for evaluation simultaneously.

### B. Parameter settings

The default population size and thread pool size were both set to 42. The search process terminated after 200 iterations. For this optimization, the number of bins  $M$  was set to 10. The boundaries of each dimension in the individual ranged from 0 to 1. The experiments in this paper were conducted with 30 independent runs, and the mean and variance were used for result analysis. The running program is written using python scripts. During the search process, the retrosynthetic route was explored using 3 NVIDIA GeForce RTX 4090 GPUs.

### C. Comparative experiment

In the experimental section, we conducted a series of comparative experiments to validate the effectiveness of the proposed algorithm. In particular, we scrutinized the impact on the number of calling single-step model, the search capability in a larger search space, and the count of feasible search solutions. Additionally, we designed several objective optimization functions and tested the algorithm's search time.

1) *Comparison experiment on calling single-step model:* The frequency of calling single-step model directly affects both the search time and search efficiency. MCTS and EA were employed to search for one, two, and three solutions for the four case products, as depicted in Table II. The values in the table indicate the average and standard deviation of the number of calling single-step model. As the number of solutions increase, both MCTS and EA require a higher count of model calls. However, EA consistently outperforms MCTS for one, two, and three solutions. Furthermore, across the four case products, the number of calling single-step model reduced

by an average of 78.6%, 59.0%, and 53.9% respectively. Consequently, EA exhibits faster search speed and higher search efficiency when compared to MCTS.

2) *Comparison experiment on the search capability:* To compare the search capabilities of the two algorithms in different search space, we conducted tests with three different beam sizes: top-10, top-15, and top-20.

Firstly, with the expansion of search space, the number of calling single-step model for both MCTS and EA increases significantly. As shown in Table III(a), due to the advantage of EA search mechanism, under the beam size of top-10, top-15, and top-20, the number of calling single-step model of EA decreased by 53.9%, 27.6%, and 16.8% on average, respectively, compared to that of MCTS based on searching 3 feasible solutions.

Secondly, this experiment is conducted with a beam size of top-10. Notably, there is a progression in the complexity of molecular structures from DemoA to DemoD, which subsequently leads to longer search time. When focusing on the same target product, the search time for EA decreased significantly compared to that of MCTS, with an average reduction of 83.9% across the four case products based on searching 3 feasible solutions, as shown in Table III(b).

Thirdly, as the search space increased in Table III(c), the complexity of the search also rises, meanwhile, the number of search routes for four case products gradually decreased under the same number of iterations. However, EA outperforms MCTS in terms of the number of search routes across top-10, top-15, and top-20. Among them, the performance on top-15 and top-20 is normal, but the performance on top-10 is particularly noteworthy, with the number of search routes increasing 5.13 times on average. This could be attributed to the relatively simplistic and easily searchable molecular structure of DemoA.

In summary, across the beam size of top-10, top-15, and top-20, EA consistently outperforms MCTS by generating a higher number of feasible search routes. Furthermore, EA demonstrates lower calling frequency of single-step model and shorter search time compared to MCTS based on searching the same feasible solutions. Overall, EA exhibits a significant improvement in search efficiency over MCTS.

3) *Comparison experiment on different objective functions:* To explore the impact of different objective functions on the

TABLE III

ANALYSIS ON SEARCH CAPABILITY (MEAN(STD.DEV.))[PERCENTAGE] ON BEAM SIZE TOP-10, TOP-15, TOP-20. PERCENTAGE IN “[·]” EXPRESSES INCREASE OR DECREASE OF EA COMPARED WITH MCTS IN THE SAME COLUMN AND UNDER THE SAME PRODUCT. DATA IN THE TABLE IS OVER 30 INDEPENDENT RUNS.

(a) Num of calling single-step model based on searching 3 feasible solutions.

Products	Method	top-10(num of calls)	top-15(num of calls)	top-20(num of calls)
DemoA	MCTS	2.74e+2(1.12e+2)	7.76e+2(3.72e+2)	9.21e+2(6.06e+2)
DemoB	MCTS	4.89e+2(3.39e+2)	7.02e+2(3.84e+2)	8.88e+2(2.29e+2)
DemoC	MCTS	3.65e+3(2.35e+3)	3.99e+3(1.98e+3)	8.00e+3(4.56e+3)
DemoD	MCTS	4.82e+3(2.00e+3)	7.29e+3(2.55e+3)	2.65e+4(3.53e+3)
DemoA	EA	8.23e+1(4.45e+1)[70.0%↓]	4.50e+2(1.18e+2)[42.0%↓]	9.62e+2(2.74e+2)[4.4%↓]
DemoB	EA	1.11e+2(5.48e+1)[77.3%↓]	3.96e+2(1.58e+2)[43.6%↓]	9.05e+2(3.95e+2)[1.9%↓]
DemoC	EA	2.41e+3(3.28e+2)[34.0%↓]	3.45e+3(6.26e+2)[13.5%↓]	7.92e+3(2.16e+3)[1.0%↓]
DemoD	EA	3.16e+3(3.45e+2)[34.4%↓]	6.47e+3(1.70e+3)[11.2%↓]	1.06e+4(1.46e+3)[60.0%↓]

(b) Search time (sec) based on searching 3 feasible solutions.

Methods	DemoA (top-10)	DemoB (top-10)	DemoC (top-10)	DemoD (top-10)
MCTS	1.63e+3(9.48e+2)	3.45e+3(3.23e+3)	1.79e+4(1.18e+4)	2.85e+4(1.12e+4)
EA	1.76e+2(5.92e+1)[89.2%↓]	3.30e+2(1.54e+2)[90.4%↓]	4.83e+3(4.50e+2)[73.0%↓]	4.85e+3(1.79e+3)[83.0%↓]

(c) Num of feasible search routes based on 200 iterations.

Products	Method	top-10(num of results)	top-15(num of results)	top-20(num of results)
DemoA	MCTS	4.00e+0(2.23e+0)	3.27e+0(1.09e+0)	2.66e+0(1.88e+0)
DemoB	MCTS	3.90e+0(0.55e+0)	3.86e+0(0.69e+0)	3.20e+0(0.92e+0)
DemoC	MCTS	3.46e+0(1.49e+0)	3.44e+0(1.16e+0)	2.88e+0(0.73e+0)
DemoD	MCTS	3.44e+0(2.36e+0)	2.60e+0(1.96e+0)	1.66e+0(0.94e+0)
DemoA	EA	8.47e+1(2.08e+1)[2017%↑]	3.86e+0(1.01e+0)[18.0%↑]	2.71e+0(1.67e+0)[1.9%↑]
DemoB	EA	4.33e+0(1.69e+0)[11%↑]	4.13e+0(0.54e+0)[7.0%↑]	3.87e+0(0.73e+0)[20.9%↑]
DemoC	EA	4.23e+0(1.24e+0)[22%↑]	3.68e+0(1.03e+0)[7.0%↑]	3.14e+0(0.75e+0)[9.0%↑]
DemoD	EA	3.60e+0(2.57e+0)[4.6%↑]	3.12e+0(2.61e+0)[20.0%↑]	1.73e+0(1.06e+0)[4.2%↑]

convergence and the ability to search feasible solutions, three objective functions are designed. Assuming there is a population of  $n$  solutions,  $\text{pop} = \{x_1, x_2, \dots, x_n\}$ , with the fitness of each solution denoted as  $f(x_i) \in (0, 1)$ . To compare the convergence of the objective functions, they are transformed into their negative counterpart. Therefore, the fitness value or selection probability of the  $i$ -th individual is designed as follows:

$$f_1 = -f(x_i) \quad (10)$$

$$f_2 = -e^{f(x_i)} \quad (11)$$

$$f_3 = -\frac{f(x_i)}{\sum_{j=1}^n f(x_j)} \quad (12)$$

During the selection process, solutions are ordered based on the magnitudes of their fitness values for  $f_1$  and  $f_2$ , with  $f_1$  is the negation of the original objective function, and  $f_2$  engineered to increase the separation between target values. Meanwhile,  $f_3$  employs the roulette wheel selection [64] sampling method, allowing for the selection of offspring solutions according to the likelihood that an individual can be sampled. Fig. 8 shows that  $f_1$  yields more feasible solutions compared to the other objective functions, making it the most effective among them. To further assess the convergence of the three different objective functions on the four case products, we normalize the value range of  $f_2$  to match the same range as  $f_1$  and  $f_3$ , which is from -1 to 0. As shown in Fig. 9,

the results clearly demonstrate that  $f_1$  outperforms the other two objective functions on DemoA, DemoB, and DemoC. Although  $f_3$  shows some similarity to  $f_1$  on DemoD,  $f_1$  still performs better after 80-th iteration.

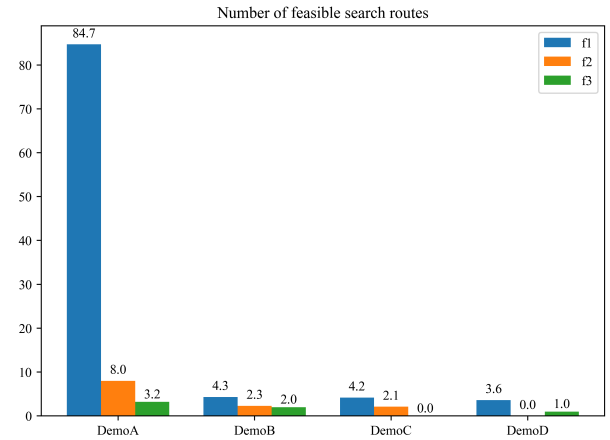


Fig. 8. The num of feasible search routes with different objective functions based on 200 iterations, over 30 independent runs.

4) Comparison experiment on search time between EA and parallel-EA: The implementation of parallel computation allowed us to expedite the running process of EA, leveraging its search mechanism effectively. The results of the final search time are depicted in Fig. 10, with the algorithm stopping at 100 epochs and being tested on four case products. Remarkably,

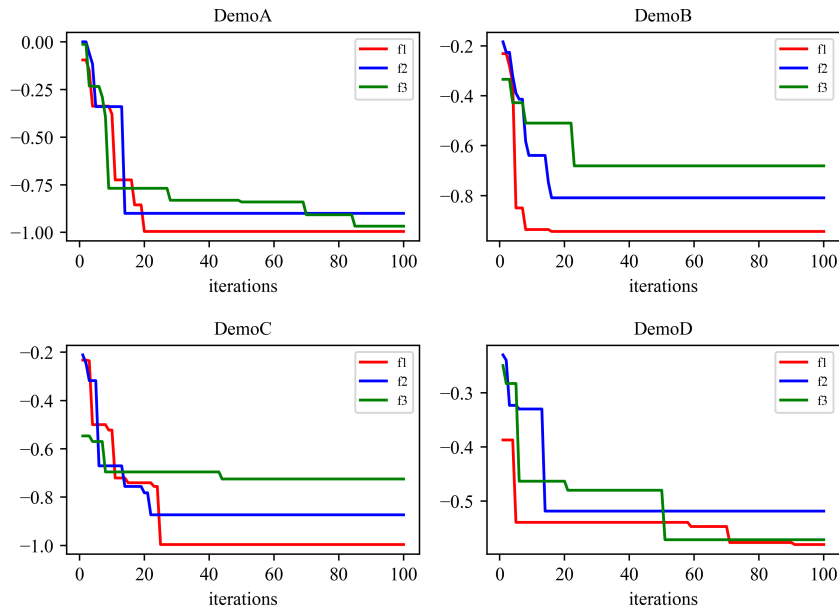


Fig. 9. Convergence curves of three different objective functions. Objective function  $f_1$  outperforms the other two functions on the four target products.

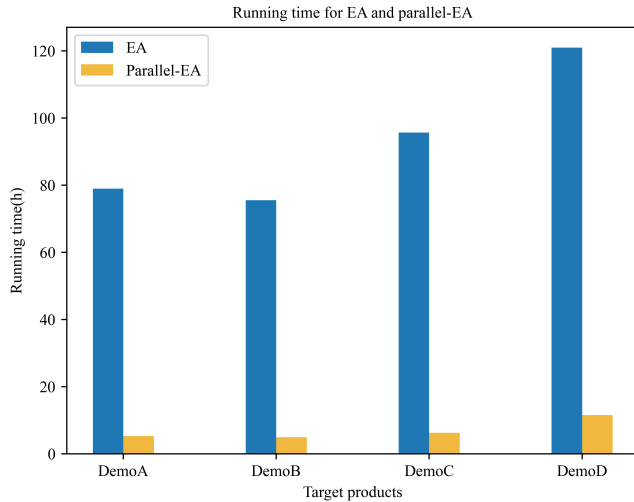


Fig. 10. Running time for EA and Parallel-EA. The algorithm stops at the maximum number of iterations 100.

the running time of parallel-EA was found to be 10-15 times faster compared to that of ordinary EA. This substantial improvement in speed demonstrates the remarkable advantage of parallel computation in accelerating the search process of EA, enabling more efficient exploration of the retrosynthetic search space.

#### D. Visualization of results

This section provides a comprehensive visual analysis of EA's performance in multi-step retrosynthesis. It includes the presentation of the retrosynthetic routes and the convergence of the population during the search process. Furthermore, EA's performance is compared with MCTS from three different perspectives.

In the retrosynthetic analysis, we used four case products that were not present in the training dataset. DemoA refers to Rufinamide [3], an antiepileptic triazole derivative. DemoB, DemoC, and DemoD are from Klucznik et al. [27], Li et al. [65], and Segler et al. [1] respectively. The retrosynthesis of these four products required 4, 2, 3, and 6 steps, respectively. As depicted in Fig. 11, DemoA's search procedure comprises four steps leading to the final products being in  $\Psi$ . The impacted functional groups are highlighted in red. The digits before and after the “.” indicate the reaction type and the substance's positioning in the results of the single-step model inference, correspondingly. These four case products have received approval from chemical experts.

During the search process, we visualized the distribution of the encoded population, as shown in Fig. 12. As the iteration increases, the population distributions gradually converge to the similar position. DemoA and DemoB demonstrate nearly rapid convergence after approximately 20 iterations, which can be attributed to their relatively simple molecular structures. In contrast, DemoC and DemoD, with more intricate molecular configurations, necessitate a broader range of reaction rules for analysis, presenting greater search challenges. As a result, these compounds converge around the 60-th iteration. Despite the intricate nature of the problem and the gradual rate of convergence, all four compounds ultimately achieve convergence.

EA consistently outperforms MCTS in different aspects, as shown in Fig. 13. In the context of identifying three feasible solutions, there is a considerable decrease in the number of calling single-step model and search time. Additionally, particularly noteworthy is EA's significant enhancement in searching feasible solutions under 200 iterations, especially for DemoA, because of its relatively simple molecular structure. Furthermore, the parallel implementation of EA results in an exponential reduction in time, making it a highly efficient

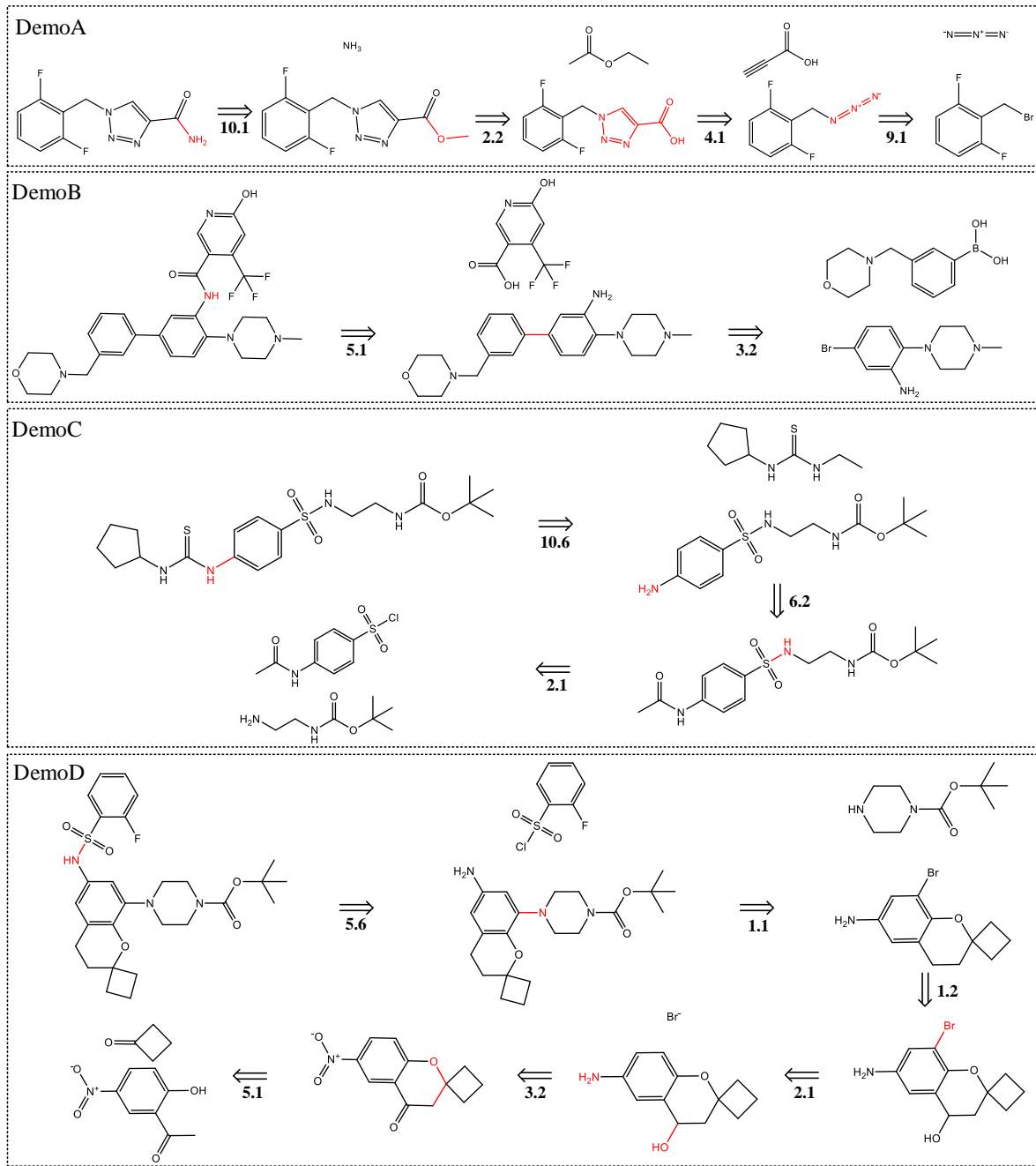


Fig. 11. Multi-step retrosynthetic routes. The affected functional groups in each step are marked red. The number before “.” and after “.” indicates the reaction class and ranking in the top-10 prediction, respectively.

approach for retrosynthetic route planning. Overall, the utilization of EA in retrosynthetic route planning demonstrates its capability to efficiently handle complex and challenging synthesis problems, thereby providing chemists with valuable and promising potential routes for target compounds.

## V. CONCLUSION

This study presents a novel and practical method for retrosynthesis of compounds, utilizing Evolutionary Algorithms (EA) for the first time to address the retrosynthetic problem. By encoding the complex retrosynthesis into an optimization problem, the retrosynthetic process is effectively simplified.

This approach allows for a well-defined search space and the establishment of a suitable objective function. At the same time, the use of parallel computation further boosts the search efficiency. According to the experimental results, the EA demonstrates a remarkable reduction in the number of calling single-step model, averaging 53.9%, when compared to the MCTS based on 3 feasible solutions. Additionally, the search time is reduced by an average of 83.9%, and the number of search routes increases by 5 times. The results demonstrate that the proposed approach significantly improves the search performance and efficiency compared to MCTS. Multiple feasible routes have been successfully discovered and

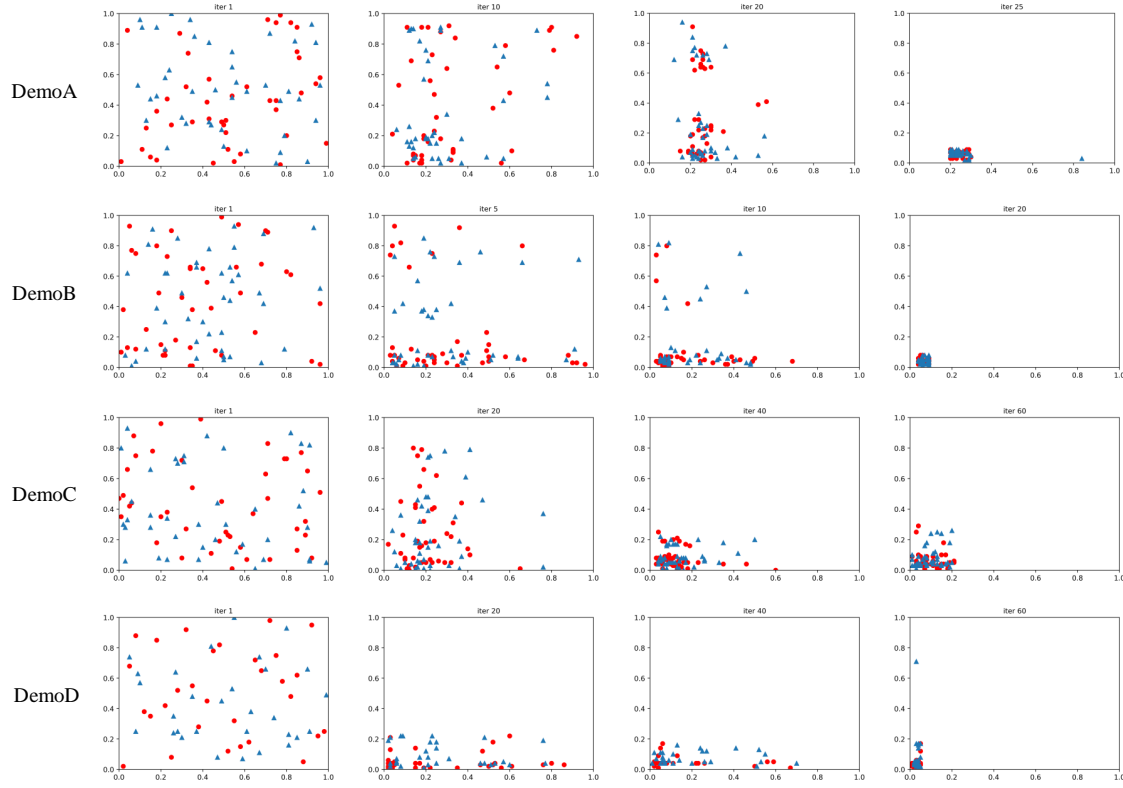


Fig. 12. The population distribution of four case products with the increase of the number of iterations. Red “o” stands for current population, and blue “ $\Delta$ ” stands for new population generated from current population.

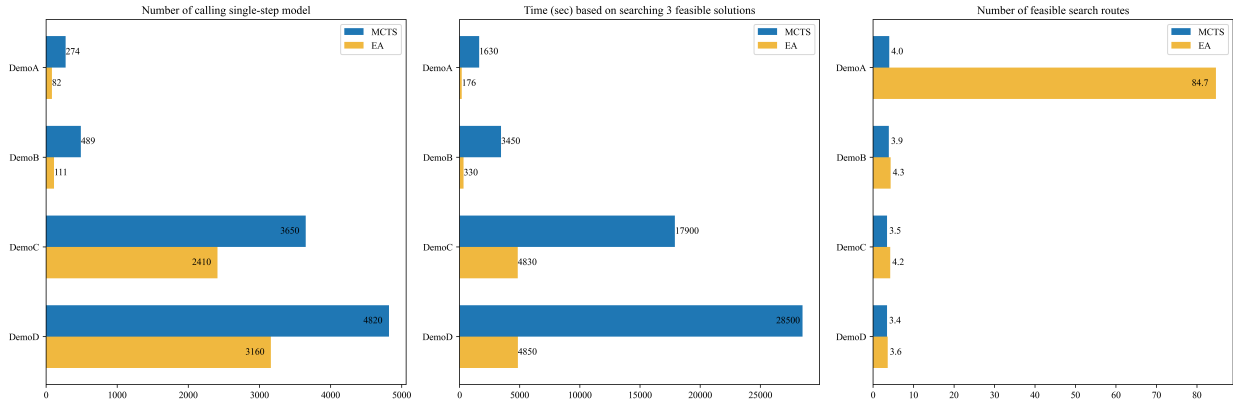


Fig. 13. The experiment of calling single-step model and search time is conducted based on identifying 3 feasible solutions. Additionally, the experiment of the number of feasible routes is carried out based on 200 iterations.

recognized by chemists, showcasing the practical utility of the method.

There are still some areas that need to be addressed in future research, for instance, in the encoding process, the proposed method converts continuous encoding search space into discrete search space for route searching. Although discrete encoding is effective in the current implementation using EA for retrosynthetic problems, there may be room for exploring more sophisticated encoding methods to further enhance search efficiency. Investigating alternative encoding techniques could potentially lead to improved performance and more efficient search processes.

## REFERENCES

- [1] M. H. Segler, M. Preuss, and M. P. Waller, “Planning chemical syntheses with deep neural networks and symbolic ai,” *Nature*, vol. 555, no. 7698, pp. 604–610, 2018.
- [2] C. W. Coley, D. A. Thomas III, J. A. Lummiss, J. N. Jaworski, C. P. Breen, V. Schultz, T. Hart, J. S. Fishman, L. Rogers, H. Gao *et al.*, “A robotic platform for flow synthesis of organic compounds informed by ai planning,” *Science*, vol. 365, no. 6453, p. eaax1566, 2019.
- [3] K. Lin, Y. Xu, J. Pei, and L. Lai, “Automatic retrosynthetic route planning using template-free models,” *Chemical Science*, vol. 11, no. 12, pp. 3355–3364, 2020.
- [4] M. Koch, T. Duigou, and J.-L. Faulon, “Reinforcement learning for bioretrosynthesis,” *ACS Synthetic Biology*, vol. 9, no. 1, pp. 157–168, 2019.

[5] G. M. B. Chaslot, M. H. Winands, and H. J. van Den Herik, "Parallel monte-carlo tree search," in *Computers and Games: 6th International Conference*. Springer, 2008, pp. 60–71.

[6] H. Dai, C. Li, C. Coley, B. Dai, and L. Song, "Retrosynthesis prediction with conditional graph logic network," *Advances in Neural Information Processing Systems*, vol. 32, 2019.

[7] R. Sun, H. Dai, L. Li, S. Kearnes, and B. Dai, "Towards understanding retrosynthesis by energy-based models," *Advances in Neural Information Processing Systems*, vol. 34, pp. 10 186–10 194, 2021.

[8] C. Yan, P. Zhao, C. Lu, Y. Yu, and J. Huang, "Retrocomposer: Composing templates for template-based retrosynthesis prediction," *Biomolecules*, vol. 12, no. 9, p. 1325, 2022.

[9] S. Zheng, J. Rao, Z. Zhang, J. Xu, and Y. Yang, "Predicting retrosynthetic reactions using self-corrected transformer neural networks," *Journal of Chemical Information and Modeling*, vol. 60, no. 1, pp. 47–55, 2019.

[10] B. Chen, T. Shen, T. S. Jaakkola, and R. Barzilay, "Learning to make generalizable and diverse predictions for retrosynthesis," *arXiv preprint arXiv:1910.09688*, 2019.

[11] I. V. Tetko, P. Karpov, R. Van Deursen, and G. Godin, "State-of-the-art augmented nlp transformer models for direct and single-step retrosynthesis," *Nature Communications*, vol. 11, no. 1, p. 5575, 2020.

[12] C. Shi, M. Xu, H. Guo, M. Zhang, and J. Tang, "A graph to graphs framework for retrosynthesis prediction," in *International Conference on Machine Learning*. PMLR, 2020, pp. 8818–8827.

[13] C. Yan, Q. Ding, P. Zhao, S. Zheng, J. Yang, Y. Yu, and J. Huang, "Retropert: Decompose retrosynthesis prediction like a chemist," *Advances in Neural Information Processing Systems*, vol. 33, pp. 11 248–11 258, 2020.

[14] V. R. Somnath, C. Bunne, C. Coley, A. Krause, and R. Barzilay, "Learning graph models for retrosynthesis prediction," *Advances in Neural Information Processing Systems*, vol. 34, pp. 9405–9415, 2021.

[15] M. E. Fortunato, C. W. Coley, B. C. Barnes, and K. F. Jensen, "Data augmentation and pretraining for template-based retrosynthetic prediction in computer-aided synthesis planning," *Journal of Chemical Information and Modeling*, vol. 60, no. 7, pp. 3398–3407, 2020.

[16] M. H. Segler and M. P. Waller, "Neural-symbolic machine learning for retrosynthesis and reaction prediction," *Chemistry—A European Journal*, vol. 23, no. 25, pp. 5966–5971, 2017.

[17] C. W. Coley, L. Rogers, W. H. Green, and K. F. Jensen, "Computer-assisted retrosynthesis based on molecular similarity," *ACS Central Science*, vol. 3, no. 12, pp. 1237–1245, 2017.

[18] S. Chen and Y. Jung, "Deep retrosynthetic reaction prediction using local reactivity and global attention," *JACS Au*, vol. 1, no. 10, pp. 1612–1620, 2021.

[19] Z. Tu and C. W. Coley, "Permutation invariant graph-to-sequence model for template-free retrosynthesis and reaction prediction," *Journal of Chemical Information and Modeling*, vol. 62, no. 15, pp. 3503–3513, 2022.

[20] Y. Wan, C.-Y. Hsieh, B. Liao, and S. Zhang, "Retroformer: Pushing the limits of end-to-end retrosynthesis transformer," in *International Conference on Machine Learning*. PMLR, 2022, pp. 22 475–22 490.

[21] X. Wang, Y. Li, J. Qiu, G. Chen, H. Liu, B. Liao, C.-Y. Hsieh, and X. Yao, "Retropprime: A diverse, plausible and transformer-based method for single-step retrosynthesis predictions," *Chemical Engineering Journal*, vol. 420, p. 129845, 2021.

[22] S.-W. Seo, Y. Y. Song, J. Y. Yang, S. Bae, H. Lee, J. Shin, S. J. Hwang, and E. Yang, "Gta: Graph truncated attention for retrosynthesis," in *Proceedings of the AAAI Conference on Artificial Intelligence*, vol. 35, no. 1, 2021, pp. 531–539.

[23] M. Sacha, M. Błaz, P. Byrski, P. Dabrowski-Tumanski, M. Chrominski, R. Loska, P. Włodarczyk-Pruszyński, and S. Jastrzebski, "Molecule edit graph attention network: modeling chemical reactions as sequences of graph edits," *Journal of Chemical Information and Modeling*, vol. 61, no. 7, pp. 3273–3284, 2021.

[24] Y. Wang, C. Pang, Y. Wang, Y. Jiang, J. Jin, S. Liang, Q. Zou, and L. Wei, "Mechretro is a chemical-mechanism-driven graph learning framework for interpretable retrosynthesis prediction and pathway planning," *arXiv preprint arXiv:2210.02630*, 2022.

[25] K. Mao, X. Xiao, T. Xu, Y. Rong, J. Huang, and P. Zhao, "Molecular graph enhanced transformer for retrosynthesis prediction," *Neurocomputing*, vol. 457, pp. 193–202, 2021.

[26] A. Heifets and I. Jurisica, "Construction of new medicines via game proof search," in *Proceedings of the AAAI Conference on Artificial Intelligence*, vol. 26, no. 1, 2012, pp. 1564–1570.

[27] T. Kluczniak, B. Mikulak-Kluczniak, M. P. McCormack, H. Lima, S. Szymkuć, M. Bhowmick, K. Molga, Y. Zhou, L. Rickershauser, E. P. Gajewska *et al.*, "Efficient syntheses of diverse, medicinally relevant targets planned by computer and executed in the laboratory," *Chem*, vol. 4, no. 3, pp. 522–532, 2018.

[28] B. Chen, C. Li, H. Dai, and L. Song, "Retro\*: learning retrosynthetic planning with neural guided a\* search," in *International Conference on Machine Learning*. PMLR, 2020, pp. 1608–1616.

[29] X. Wang, Y. Qian, H. Gao, C. W. Coley, Y. Mo, R. Barzilay, and K. F. Jensen, "Towards efficient discovery of green synthetic pathways with monte carlo tree search and reinforcement learning," *Chemical Science*, vol. 11, no. 40, pp. 10 959–10 972, 2020.

[30] J. H. Holland, *Adaptation in natural and artificial systems: an introductory analysis with applications to biology, control, and artificial intelligence*. MIT Press, 1992.

[31] R. Storn and K. Price, "Differential evolution-a simple and efficient heuristic for global optimization over continuous spaces," *Journal of Global Optimization*, vol. 11, no. 4, p. 341, 1997.

[32] J. Kennedy and R. Eberhart, "A new optimizer using particle swarm theory. in proceedings of the sixth international symposium on micro machine and human science. nagoya japon," *IEEE Service Center Piscataway, NJ*, 1995.

[33] H.-P. P. Schwefel, *Evolution and optimum seeking: the sixth generation*. John Wiley & Sons, Inc., 1993.

[34] D. B. Fogel, *Evolutionary computation: toward a new philosophy of machine intelligence*. John Wiley & Sons, 2006.

[35] X. Yao, Y. Liu, and G. Lin, "Evolutionary programming made faster," *IEEE Transactions on Evolutionary Computation*, vol. 3, no. 2, pp. 82–102, 1999.

[36] J. R. Koza, "Genetic programming as a means for programming computers by natural selection," *Statistics and Computing*, vol. 4, pp. 87–112, 1994.

[37] P. Larrañaga and J. A. Lozano, *Estimation of distribution algorithms: A new tool for evolutionary computation*. Springer Science & Business Media, 2001, vol. 2.

[38] H. Mühlenbein and G. Paass, "From recombination of genes to the estimation of distributions i. binary parameters," in *Parallel Problem Solving from Nature*. Springer, 1996, pp. 178–187.

[39] J. De Bonet, C. Isbell, and P. Viola, "Mimic: Finding optima by estimating probability densities," *Advances in Neural Information Processing Systems*, vol. 9, 1996.

[40] D. Heckerman, D. Geiger, and D. M. Chickering, "Learning bayesian networks: The combination of knowledge and statistical data," *Machine Learning*, vol. 20, pp. 197–243, 1995.

[41] R. Etxeberria, "Global optimization using bayesian networks," in *Proc. 2nd Symposium on Artificial Intelligence (CIMAF-99)*, 1999.

[42] M. Pelikan, K. Sastry, and D. E. Goldberg, "Multiobjective hbo, clustering, and scalability," in *Proceedings of the 7th Annual Conference on Genetic and Evolutionary Computation*, 2005, pp. 663–670.

[43] M. Pelikan and M. Pelikan, *Hierarchical Bayesian optimization algorithm*. Springer, 2005.

[44] R. Santana, P. Larrañaga, and J. A. Lozano, "Learning factorizations in estimation of distribution algorithms using affinity propagation," *Evolutionary Computation*, vol. 18, no. 4, pp. 515–546, 2010.

[45] M. Laumanns and J. Ocenasek, "Bayesian optimization algorithms for multi-objective optimization," in *Parallel Problem Solving from Nature*. Springer, 2002, pp. 298–307.

[46] K. Deb, A. Pratap, S. Agarwal, and T. Meyarivan, "A fast and elitist multiobjective genetic algorithm: Nsga-ii," *IEEE Transactions on Evolutionary Computation*, vol. 6, no. 2, pp. 182–197, 2002.

[47] Q. Zhang, A. Zhou, and Y. Jin, "Rm-med: A regularity model-based multiobjective estimation of distribution algorithm," *IEEE Transactions on Evolutionary Computation*, vol. 12, no. 1, pp. 41–63, 2008.

[48] Y. Jin and B. Sendhoff, "Connectedness, regularity and the success of local search in evolutionary multi-objective optimization," in *The 2003 Congress on Evolutionary Computation, 2003. CEC'03.*, vol. 3. IEEE, 2003, pp. 1910–1917.

[49] S. Baluja, "Population-based incremental learning. a method for integrating genetic search based function optimization and competitive learning," *Carnegie-Mellon Univ Pittsburgh Pa Dept Of Computer Science, Tech. Rep.*, 1994.

[50] M. Pelikan, D. E. Goldberg, and E. Cantu-Paz, "Linkage problem, distribution estimation, and bayesian networks," *Evolutionary Computation*, vol. 8, no. 3, pp. 311–340, 2000.

[51] M. Pelikan and H. Mühlenbein, "The bivariate marginal distribution algorithm," in *Advances in Soft Computing: Engineering Design and Manufacturing*. Springer, 1999, pp. 521–535.

- [52] P. A. Bosman and D. Thierens, "Multi-objective optimization with the naive midea," *Studies in Fuzziness and Soft Computing*, vol. 192, p. 123, 2006.
- [53] J. Ocenasek, S. Kern, N. Hansen, and P. Koumoutsakos, "A mixed bayesian optimization algorithm with variance adaptation," in *Parallel Problem Solving from Nature*. Springer, 2004, pp. 352–361.
- [54] L. Zhang, H. Yang, S. Yang, and X. Zhang, "A macro-micro population-based co-evolutionary multi-objective algorithm for community detection in complex networks [research frontier]," *IEEE Computational Intelligence Magazine*, vol. 18, no. 3, pp. 69–86, 2023.
- [55] T. Back, M. Emmerich, and O. Shir, "Evolutionary algorithms for real world applications [application notes]," *IEEE Computational Intelligence Magazine*, vol. 3, no. 1, pp. 64–67, 2008.
- [56] L. Weber, "Multi-component reactions and evolutionary chemistry," *Drug Discovery Today*, vol. 7, pp. 143–147, 2002.
- [57] D. S. Wigh, J. M. Goodman, and A. A. Lapkin, "A review of molecular representation in the age of machine learning," *Computational Molecular Science*, vol. 12, no. 5, p. e1603, 2022.
- [58] A. Mullard *et al.*, "The drug-maker's guide to the galaxy," *Nature*, vol. 549, no. 7673, pp. 445–447, 2017.
- [59] A. Cereto-Massagué, M. J. Ojeda, C. Valls, M. Mulero, S. Garcia-Vallvé, and G. Pujadas, "Molecular fingerprint similarity search in virtual screening," *Methods*, vol. 71, pp. 58–63, 2015.
- [60] G. Landrum *et al.*, "Rdkit: A software suite for cheminformatics, computational chemistry, and predictive modeling," *Greg Landrum*, vol. 8, 2013.
- [61] A. Zhou, J. Sun, and Q. Zhang, "An estimation of distribution algorithm with cheap and expensive local search methods," *IEEE Transactions on Evolutionary Computation*, vol. 19, no. 6, pp. 807–822, 2015.
- [62] B. Liu, B. Ramsundar, P. Kawthekar, J. Shi, J. Gomes, Q. Luu Nguyen, S. Ho, J. Sloane, P. Wender, and V. Pande, "Retrosynthetic reaction prediction using neural sequence-to-sequence models," *ACS Central Science*, vol. 3, no. 10, pp. 1103–1113, 2017.
- [63] C. W. Coley, L. Rogers, W. H. Green, and K. F. Jensen, "Sescore: synthetic complexity learned from a reaction corpus," *Journal of Chemical Information and Modeling*, vol. 58, no. 2, pp. 252–261, 2018.
- [64] A. Lipowski and D. Lipowska, "Roulette-wheel selection via stochastic acceptance," *Physica A: Statistical Mechanics and its Applications*, vol. 391, no. 6, pp. 2193–2196, 2012.
- [65] C. Li, X. Deng, W. Zhang, X. Xie, M. Conrad, Y. Liu, J. P. F. Angeli, and L. Lai, "Novel allosteric activators for ferroptosis regulator glutathione peroxidase 4," *Journal of Medicinal Chemistry*, vol. 62, no. 1, pp. 266–275, 2018.